Neuropathic pain-alleviating activity of novel 5-HT6 receptor inverse agonists derived from 2-aryl-1H-pyrrole-3-carboxamide

Marcin Drop, Florian Jacquot, Vittorio Canale, Séverine Chaumont-Dubel, Maria Walczak, Grzegorz Satala, Klaudia Nosalska, Gilbert Umuhire Mahoro, Karolina Sloczyńska, Kamil Piska, et al.

Bioorganic Chemistry 115 (2021) 105218

Contents lists available at ScienceDirect

Bioorganic Chemistry

journal homepage: www.elsevier.com/locate/bioorg

Neuropathic pain-alleviating activity of novel 5-HT$_6$ receptor inverse agonists derived from 2-aryl-1*H*-pyrrole-3-carboxamide

Marcin Drop [a,b], Florian Jacquot [e], Vittorio Canale [a], Severine Chaumont-Dubel [c], Maria Walczak [a], Grzegorz Satała [d], Klaudia Nosalska [a], Gilbert Umuhire Mahoro [b], Karolina Słoczyńska [a], Kamil Piska [a], Sylvain Lamoine [e], Elżbieta Pękala [a], Nicolas Masurier [b], Andrzej J. Bojarski [d], Maciej Pawłowski [a], Jean Martinez [b], Gilles Subra [b], Xavier Bantreil [b], Frédéric Lamaty [b], Alain Eschalier [e], Philippe Marin [c], Christine Courteix [e], Paweł Zajdel [a,*]

[a] Faculty of Pharmacy, Jagiellonian University Medical College, 9 Medyczna Str., 30-688 Kraków, Poland
[b] IBMM, Université de Montpellier, CNRS, ENSCM, 34095 Montpellier, France
[c] Institut de Génomique Fonctionelle, Université de Montpellier, CNRS INSERM, 34094 Montpellier, France
[d] Maj Institute of Pharmacology, Polish Academy of Sciences, 12 Smętna Str., 31-343 Kraków, Poland
[e] Université Clermont Auvergne, INSERM U1107, NEURO-DOL, F-63000 Clermont-Ferrand, France

ARTICLE INFO

Keywords:
Neuropathic pain
5-HT$_6$ receptor inverse agonism
Cdk5 signaling
mTOR kinase
Spinal nerve ligation
Flow chemistry

ABSTRACT

The diverse signaling pathways engaged by serotonin type 6 receptor (5-HT$_6$R) together with its high constitutive activity suggests different types of pharmacological interventions for the treatment of CNS disorders. Non-physiological activation of mTOR kinase by constitutively active 5-HT$_6$R under neuropathic pain conditions focused our attention on the possible repurposing of 5-HT$_6$R inverse agonists as a strategy to treat painful symptoms associated with neuropathies of different etiologies. Herein, we report the identification of compound **33** derived from the library of 2-aryl-1*H*-pyrrole-3-carboxamides as a potential analgesic agent. Compound **33** behaves as a potent 5-HT$_6$R inverse agonist at Gs, Cdk5, and mTOR signaling. Preliminary ADME/Tox studies revealed preferential distribution of **33** to the CNS and placed it in the low-risk safety space. Finally, compound **33** dose-dependently reduced tactile allodynia in spinal nerve ligation (SNL)-induced neuropathic rats.

1. Introduction

Neuropathic pain is a significant public health concern worldwide. According to the International Association for the Study of Pain, 5–10% of adults are affected by chronic pain of neuropathic origin [1,2], resulting from a lesion or a disease affecting the central or peripheral somatosensory nervous system [3–5]. First-line treatments such as serotonin-noradrenaline reuptake inhibitors (SNRIs, duloxetine and venlafaxine), gabapentin, tricyclic antidepressants, and topical agents (for peripheral neuropathic pain) are only partially effective as revealed by their NNT (number of patients who needed to be treated to obtain a 50% pain relief in one patient) values ranging from 3.6 to 7.7 [6,7]. An increasing body of evidence supports both pronociceptive and anti-nociceptive effects of serotonin and proposes serotonin type 6 receptor (5-HT$_6$R) as a potential target for new analgesic agents [8–10].

5-HT$_6$R belongs to the family of G-protein-coupled receptors (GPCRs). In addition to the canonical Gs-adenylyl cyclase pathway, it recruits several cellular signaling cascades such as extracellular signal-regulated kinase (ERK)1/2, cyclin-dependent kinase 5 (Cdk5), and mechanistic target of rapamycin (mTOR) pathways [11]. Of note, 5-HT$_6$R shows a high level of ligand-independent constitutive activity for both recombinant receptors in cell lines [12] and native receptors in primary cultured neurons [13].

Apart from high abundance of the 5-HT$_6$R in the brain regions responsible for cognitive functions, it is also expressed in excitatory interneurons of the dorsal spinal cord [14] and is involved in tactile perception. Thus, as an addition to a well-documented beneficial effect of 5-HT$_6$R antagonists on cognition [15–19], recent studies have established that 5-HT$_6$R blockade with SB-258585 or pyrazolo[3,4] pyridine-7-one and 1-aryl-5-isopropyl-pyrazole derivatives produces antiallodynic effect in neuropathic rats [20–22].

The mechanisms underlying the antinociceptive effects of 5-HT$_6$R

* Corresponding author at: Department of Organic Chemistry, Jagiellonian University Medical College, Poland.
E-mail address: pawel.zajdel@uj.edu.pl (P. Zajdel).

https://doi.org/10.1016/j.bioorg.2021.105218
Received 31 May 2021; Received in revised form 16 July 2021; Accepted 24 July 2021
Available online 29 July 2021

antagonists remain unclear. We have recently demonstrated that these effects might result from blockade of mTOR activation by constitutively active spinal 5-HT$_6$Rs [10]. These observations are consistent with studies that identified mTOR kinase as a crucial regulator of central and peripheral pain sensitization [23,24] and demonstrated that its inhibition by rapamycin produces analgesic effects in a wide range of pain-related paradigms in rodents [25–27].

In the present study, we describe a systematic structure–activity relationship (SAR) to provide a small library of 5-HT$_6$R inverse agonists in a group of 2-aryl-1*H*-pyrrole-3-carboxamide to obtain 5-HT$_6$R inverse agonists that exhibit analgesic effects in neuropathic pain. Structural diversity originates from variation of the alicyclic amines in the 3-carboxamide fragment (**R^3**), functionalizing a phenyl moiety (**R^2**) linked with *N*^{1}-pyrrole by a sulfonyl group or a methylene bridge (**X = SO$_2$** or **CH$_2$**), and introducing substituents at the 2-phenyl ring of the pyrrole fragment or its replacement with naphth-2-yl or heteroaryl moieties (**Ar**) (Fig. 1).

Furthermore, we show that compound **33** inhibits agonist-independent 5-HT$_6$R-operated activation of Gs, Cdk5, and mTOR signaling, and that it reduces tactile allodynia in spinal nerve ligation (SNL)-induced neuropathic rats.

2. Results and discussion

2.1. Chemistry

The designed compounds were synthesized starting from 2-aryl-1*H*-pyrrole-3-carboxylic acids **7a–k** (Scheme 1). The key β-aminoester (**1a–i**) and diene intermediates (**4a–i**) bearing substituted phenyl or naphth-2-yl moieties in **Ar** were synthesized by a two-step approach involving an *aza*-Baylis-Hillman reaction and *N*-allylation as previously reported [28]. An alternative synthetic route was required to prepare dienes bearing heteroaryl fragments, namely pyridin–2–yl (**4j**) and thien–2–yl (**4k**), as the corresponding *aza*-Baylis-Hillman reaction failed. Thus, a three-step synthesis was envisioned, consisting of Baylis-Hillman reaction of methylacrylate and heteroaryl aldehydes to provide alcohols **2j–k**, which were subsequently converted into their corresponding acetates **3j–k**. The final nucleophilic substitution performed directly with *N*-allyl-tosylamine yielded an undesired isomer of **4j-k**, originating from a S$_N$2′ reaction of the amine on the allylic acetate. Hence, a first S$_N$2′ with DABCO, followed by a second S$_N$2′ with *N*-allyl-tosylamine was necessary to yield the desired dienes **4j–k**, as reported in the literature with other tosylamines [29]. Next, continuous flow ring-closing metathesis (RCM) was performed in the presence of ruthenium catalyst **M2** according to our previously reported procedure [30]. Of note, the *N*-containing heterocyclic compounds, especially pyridines, are generally more difficult substrates in RCM, because the nitrogen atom might coordinate with the ruthenium centre and poison the catalyst. Thus, HCl was used for the flow RCM of **4j** to protonate the pyridine and obtain **5j**. Then, removal of the tosyl protection group in the presence of sodium *tert*-butoxide (NaO*t*Bu) with simultaneous aromatization yielded the 2-substituted-1*H*-pyrrole-3-methylcarboxylates **6a–k**. They were subsequently hydrolyzed to their corresponding carboxylic acids (**7a–k**) in a refluxing aqueous solution of NaOH.

Subsequently, appropriate acids (**7a–k**) were reacted with diverse Boc-protected alicyclic diamines in the presence of 1–hydroxybenzotriazole (HOBt), benzotriazole-1-yl-oxy-tris-(dimethylamino)-phosphonium hexafluorophosphate (BOP), and triethylamine. The obtained carboxamides (**8a–r**) were coupled with diverse phenylsulfonyl chlorides or 3-chlorobenzyl bromide under basic conditions (phosphazene base P_1-*t*-Bu-tris(tetramethylene), BTPP) to provide *N*^{1}-substituted 2-arylpyrrole-3-carboxamides. Final treatment with methanolic HCl yielded the target compounds **9–37** as appropriate hydrochloride salts (Scheme 2).

2.2. Structure-activity relationship studies

Motivated by our previous results, we decorated the central framework of 2-phenyl-1*H*-pyrrole-3-carboxamide [28] with diverse alicyclic amines at the 3-carboxamide fragment. The affinity of final compounds **9–37** for 5-HT$_6$R was determined using the [^{3}H]-LSD binding assay in HEK293 cells stably expressing human 5-HT$_6$R [31]. The initial results revealed that introducing a methylene bridge between the amide bond and the pyrrolidin-3-yl moiety (**9**, **10**) reduced the affinity for the target receptor. Further replacement of the pyrrolidin-3-yl fragment with its homologs, i.e., both enantiomers of piperidin-3-yl (**11**, **12**), was also not favorable. Only structural rearrangement around the piperidine moiety – a shift of the protonable nitrogen atom to the distal position of the amide bond – increased the affinity for 5-HT$_6$R (**11**, **12** *vs.* **13**). Finally, the introduction of the bicyclic (1*R*,5*S*)-8-azabicyclo[3.2.1]octan-3-yl fragment (**14**) as well as piperazinyl (**15**) or 1,4-diazacycloheptanyl (**16**) was not favorable for the interaction with 5-HT$_6$R (Table 1).

In accordance with our previous studies indicating that substitution of the phenylsulfonyl fragment in the *C*^{3} position with small-size halogens stabilizes the ligand-receptor complex through the formation of a halogen bond (chlorine) or dipole–dipole, van der Waals interaction (fluorine) [28,33,34], we only introduced these atoms (alone or in combinations) in **R^2**. As expected, the functionalization of the *N*^{1}-phenylsulfonyl ring in the *C*^{3} position improved the affinity of compounds, with the highest affinity for 5-HT$_6$R observed for the chlorine-substituted compound (**18**, K_i = 28 nM). In contrast, the introduction of two electron-withdrawing substituents (**20–24**) was not beneficial for the interaction with 5-HT$_6$R as compared to monohalo-substituted derivatives (**17–18**) or even an unsubstituted derivative (**13**) (Table 2).

Inasmuch a structural functionalization of the 2-phenyl ring at the pyrrole moiety might affect the affinity for 5-HT$_6$R, selected

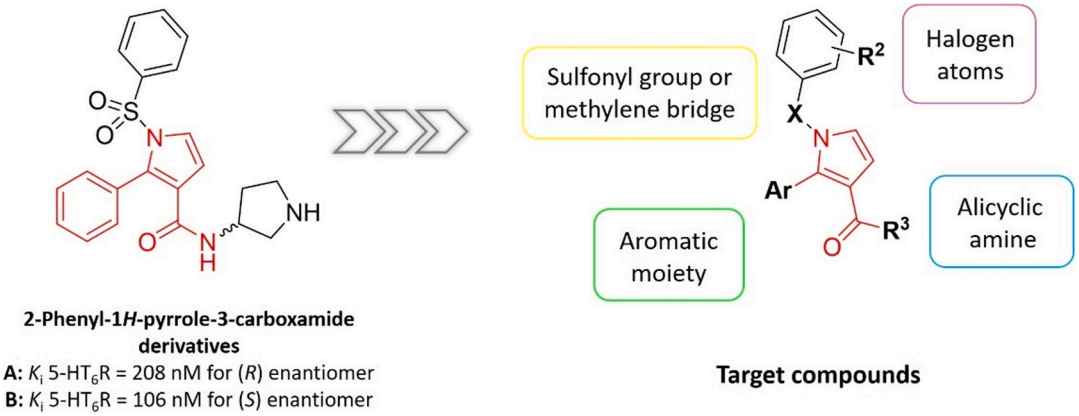

Fig. 1. The scope of structural functionalization of 2-aryl-1*H*-pyrrole-3-carboxamide scaffold providing the target compounds.

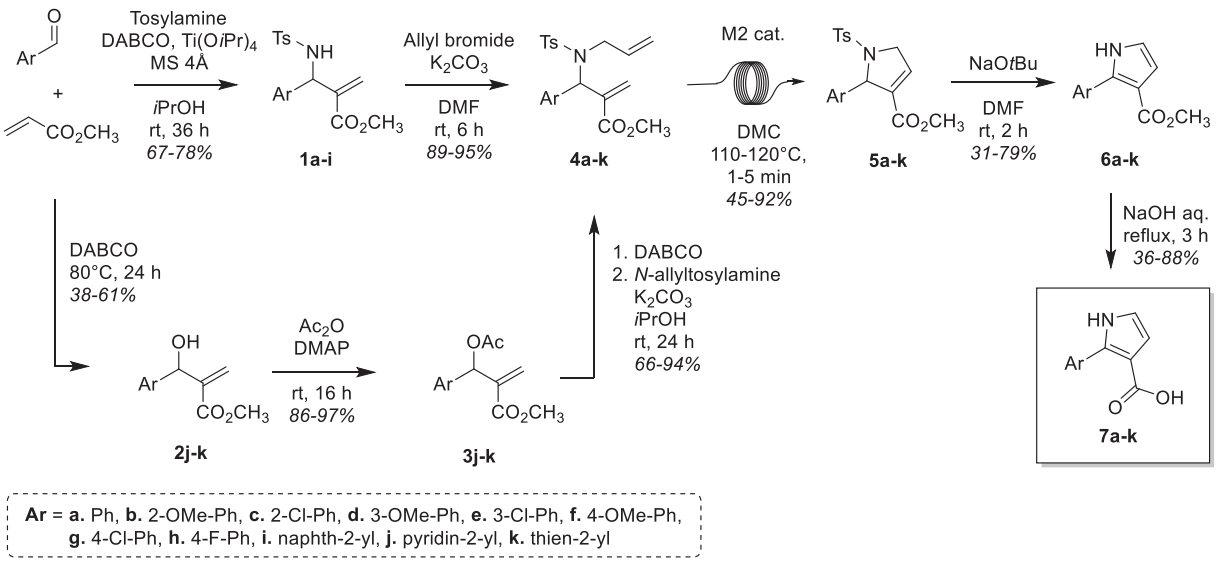

Scheme 1. Synthetic route for the preparation of 2-aryl-1*H*-pyrrole-3-carboxylic acids (**7a–k**).

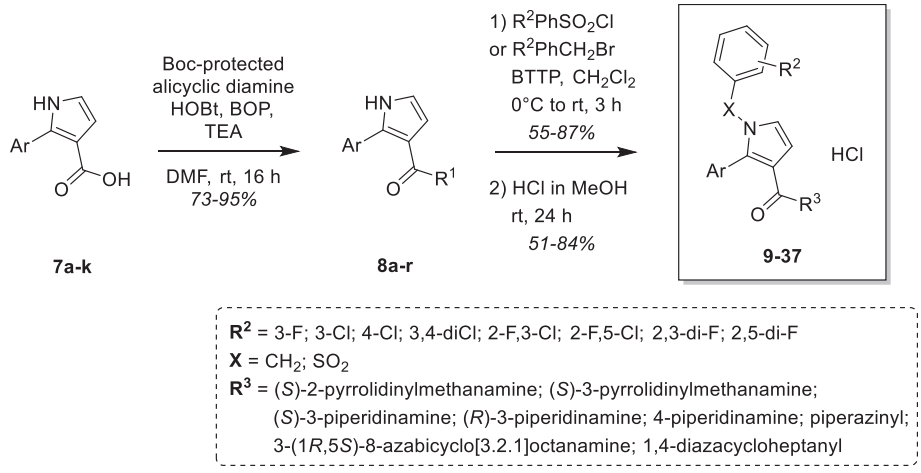

Scheme 2. General synthetic route for the preparation of final compounds **9–37** obtained as hydrochloride salts.

substituents, namely methoxy group, chlorine, and fluorine, were introduced (Table 3). Regardless of the position in the 2-phenyl ring, the introduction of an electron-donating methoxy group decreased the affinity for 5-HT$_6$R (**13** *vs.* **25**, **27**, **29**) up to 8-fold. Among the electron-withdrawing atoms, chlorine in C^3 and C^4 position slightly increased the affinity of compounds for the receptor (**13** *vs.* **28**, **30**). In line with published results [28], a fluorine atom in C^4 position was also beneficial for the interaction with 5-HT$_6$R (**13** *vs.* **31**, **17** *vs.* **32**, **18** *vs.* **33**). Furthermore, the replacement of the 2-phenyl ring at the pyrrole moiety with naphthyl (**18** *vs.* **34**) or heteroaryl moieties, i.e., pyridine-2-yl, thien-2-yl (**18** *vs.* **35**, **36**), decreased the affinity for 5-HT$_6$R. The SAR studies revealed the same trend when the sulfonyl group in N^1 position was replaced by a methylene bridge (**33** *vs.* **37**) (Table 3).

Finally, our SAR analysis selected compound **33**, which shows the highest affinity for 5-HT$_6$R (K_i = 23 nM) and does not bind to 5-HT$_{1A}$ (K_i = 72420 nM), 5-HT$_{2A}$ (K_i = 98510 nM), 5-HT$_7$ (K_i = 1858 nM), and dopamine D$_2$ (K_i = 7807 nM) receptors.

2.3. *Effect of compound **33** on 5-HT$_6$R-elicited signaling pathways*

Considering the ability of 5-HT$_6$R to adopt unique conformations engaging different signaling pathways, we next examined the effect of compound **33** on the recruitment of the canonical Gs-adenylyl cyclase pathway and noncanonical pathways, i.e., Cdk5 and mTOR kinases.

2.3.1. *5-HT$_6$R-dependent Gs signaling*

The effect of compound **33** on G-s-mediated adenylate cyclase activity was determined in 1321N1 cells expressing 5-HT$_6$R. Compound **33** decreased 5-carboxamidotryptamine (5-CT)-induced cAMP production, thus classifying this molecule as a 5-HT$_6$R antagonist (K_b = 6.62 nM) (Table 4).

The high level of 5-HT$_6$R constitutive activity, corresponding to spontaneous activity of the receptor in the absence of an agonist occupancy, provides the pharmacological distinction between inverse agonists and neutral antagonists [35]. The effect of **33** on the agonist-independent 5-HT$_6$R-elicited Gs signaling pathway was tested in NG108-15 cells transiently expressing the receptors. Compound **33** strongly decreased the cAMP level in a concentration-dependent

Table 1

Binding data of synthesized compounds **9**–**16** and references **A**, **B** for 5-HT$_6$R.

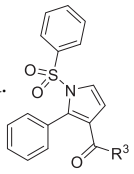

No	R^3	R/S	K_i [nM] [a] 5-HT$_6$R
A [b]	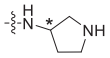	*R*	208 ± 23
B [b]		*S*	106 ± 5
9	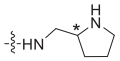	*S*	225 ± 18
10	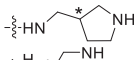	*S*	221 ± 15
11	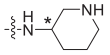	*S*	648 ± 92
12		*R*	790 ± 127
13	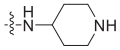		47 ± 3
14	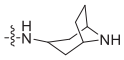		593 ± 64
15			2362 ± 359
16	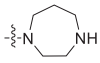		4086 ± 759
SB-271046 [c]			1.2

[a] Mean K_i values ± SEM are reported for three independent experiments in HEK293 cells.
[b] Data taken from [28] where **A** is encoded as **7**, and **B** is encoded as **8**.
[c] Data taken from [32].

Table 2

Binding data of synthesized compounds **17**–**24** for 5-HT$_6$R.

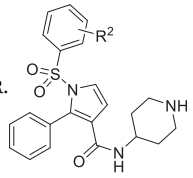

No	R^2	K_i [nM] [a] 5-HT$_6$R
17	3-F	30 ± 2
18	3-Cl	28 ± 4
19	4-Cl	1116 ± 193
20	3,4-diCl	517 ± 85
21	2-F,3-Cl	108 ± 7
22	2-F,5-Cl	233 ± 29
23	2,3-di-F	427 ± 20
24	2,5-di-F	248 ± 18

[a] Mean K_i values ± SEM are reported for three independent experiments in HEK293 cells.

manner; this was reminiscent of the effect of the reference 5-HT$_6$R inverse agonist SB-271046 (Fig. 2), and the compound was defined as an inverse agonist. Strikingly, compound **33** produced a stronger inhibition of basal cAMP production than SB-271046 (75.52% ± 3.5% inhibition *vs.* 82.73% ± 6.2% inhibition measured at the maximally effective concentrations of SB-271046 and compound **33**, respectively).

2.3.2. 5-HT$_6$R-operated Cdk5 signaling

5-HT$_6$R is also capable of activating Cdk5 signaling in an agonist-independent manner in NG108-15 cells, a process that promotes neurite growth and NG108-15 cell differentiation. Exposure of NG108-15 cells to compound **33** or SB-271046 significantly reduced neurite length, thus indicating that both compounds also behave as inverse agonists of 5-HT$_6$R at Cdk5 signaling (Fig. 3).

2.3.3. 5-HT$_6$R-operated mTOR signaling

5-HT$_6$R recruits mTORC1 and stimulates mTOR through a dual mechanism involving the canonical PI3K/Akt/Tsc1,2/Rheb pathway and a physical interaction between the receptor's C-terminal domain and mTOR [11]. mTOR is a serine/threonine kinase that plays a crucial role regulating protein synthesis and thus controls many basic physiological functions, including pain modulation and transmission [23,36–38]. In addition, mTOR and its downstream effectors were found in the central regions involved in the nociception process, such as the dorsal root ganglion and spinal cord dorsal horn [39]. Further body of evidence confirmed that the mTOR inhibitor rapamycin produces analgesic effects in traumatic [26], chemically (bortezomib) [27], and diabetes (streptozotocin)-induced [40] neuropathy in rats.

Our recent investigations demonstrated that the basal level of mTOR phosphorylation at Ser2448 in HEK-293 cells expressing 5-HT$_6$Rs was significantly reduced by 5-HT$_6$R inverse agonists, i.e., SB-258585, but

Table 3

Binding data of synthesized compounds **25**–**37** for 5-HT_6R.

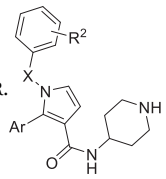

No	Ar	R^2	X	K_i [nM] [a] 5-HT_6R
25	2-OCH_3-Ph	H	SO_2	793 ± 47
26	2-Cl-Ph	H	SO_2	76 ± 11
27	3-OCH_3-Ph	H	SO_2	166 ± 9
28	3-Cl-Ph	H	SO_2	38 ± 3
29	4-OCH_3-Ph	H	SO_2	385 ± 17
30	4-Cl-Ph	H	SO_2	41 ± 5
31	4-F-Ph	H	SO_2	36 ± 4
32	4-F-Ph	3-F	SO_2	28 ± 2
33	4-F-Ph	3-Cl	SO_2	23 ± 3
34	naphth-2-yl	3-Cl	SO_2	76 ± 5
35	pyridin-2-yl	3-Cl	SO_2	142 ± 15
36	thien-2-yl	3-Cl	SO_2	83 ± 4
37	4-F-Ph	3-Cl	CH_2	154 ± 10

[a] Mean K_i values ± SEM are reported for three independent experiments in HEK293 cells.

Table 4
The property of compound **33** in 1321N1 cells and its functional activity at 5-HT_6R-dependent Gs signaling in NG108-5 cells.

Compound	K_i [nM] [a] 5-HT_6R	K_b [nM] [b] 5-HT_6R	IC_{50} [nM] [c] Gs signaling	Functional profile
33	23	6.62	164	Inverse agonist
SB–271046	1.2[d]	1.95[d]	98	Inverse agonist

[a] Mean K_i values (SEM ± 20%) are reported for three independent experiments in HEK293 cells.
[b] Mean K_b values (SEM ± 15%) are reported for three independent experiments in 1321N1 cells.
[c] Mean IC_{50} values (SEM ± 18%) are reported for three independent experiments in NG108-15 cells.
[d] Data taken from [32].

not by neutral antagonists i.e., IIQ, CPPQ [10]. Further studies showed that inhibiting mTOR activation by constitutively active 5-HT_6R alleviates painful symptoms in neuropathic pain models of different etiologies.

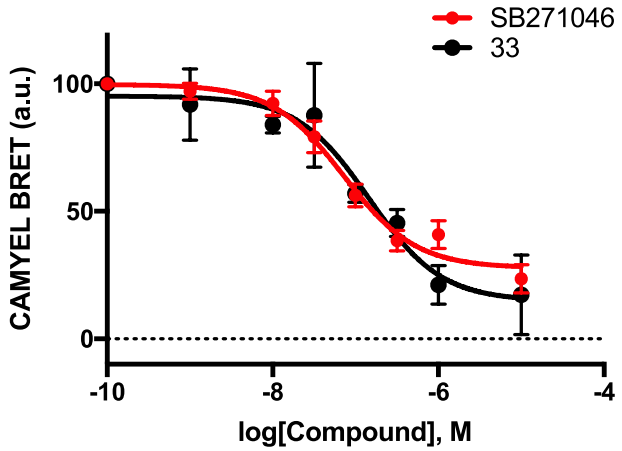

Fig. 2. Inhibition of basal cAMP production in NG108-15 cells transiently transfected with 5-HT_6Rs by compound **33** and SB–271046. Each point represents the mean ± SEM of the BRET values obtained from quadruplicates measurements in three independent experiments made in different sets of cultured cells.

In line with these observations, we also investigated the effect of compound **33** administration to rats on mTOR signaling in the brain by immunohistochemistry using antibodies against ribosomal protein S6 phosphorylated on $Ser^{240/244}$, a downstream target of mTOR. The administration of compound **33** strongly decreased the level of phosphorylated S6 in the prefrontal cortex, a brain structure involved in the modulation of cognitive processes by 5-HT_6R (Fig. 4). These observations suggest that compound **33** might be a promising treatment agent for neuropathic pain.

2.4. Preliminary ADME/Tox and pharmacokinetics characterization

Because the assessment of *in vitro* ADME/Tox properties of novel bioactive compounds is a key step in the preclinical lead optimization process, we conducted biotransformation studies of compound **33** by using rat liver microsomes (RLM). Compound **33** exhibited a low value of intrinsic clearance (8.5 μL/min/mg), indicating its high metabolic stability. Additionally, compound **33** exhibited high solubility and chemical stability in a wide pH range (Table 5).

Compound **33** was tested in the human neuroblastoma (SH-SY5Y) and human hepatocellular carcinoma (HepG2) cellular models to exclude potential cytotoxic effects. We investigated the metabolic activity of cells in the MTT test by using doxorubicin (DOX) as a positive control. Compound **33** did not induce neurotoxicity, nor hepatotoxicity. Compound **33** also did not cause significant changes in the number of micronuclei, dicentric bridges as well as nuclear buds, thus indicating the absence of genotoxicity (more details in Supplementary Information; SI: 11, 12).

The PK profile of compound **33** was determined in male Wistar rats after single intragastric gavage (*i.g.*) at the dose of 10 mg/kg. Compound **33** was slowly absorbed from the gastrointestinal tract with t_{max} = 60 min; it achieved a concentration of 216.6 ng/mL in plasma but crucially crossed the blood–brain barrier, reaching the C_{max} (436.6 ng/mL) in the brain after 30 min. Compound **33** displayed high distribution to the brain, with the brain/plasma ratio of 2.18 (Table 6), and it was eliminated very slowly from the brain, showing a long half-life time of 29 h.

2.5. Neuropathic pain alleviating properties of compound *33*

Since we have previously shown that 5-HT_6R inverse agonists

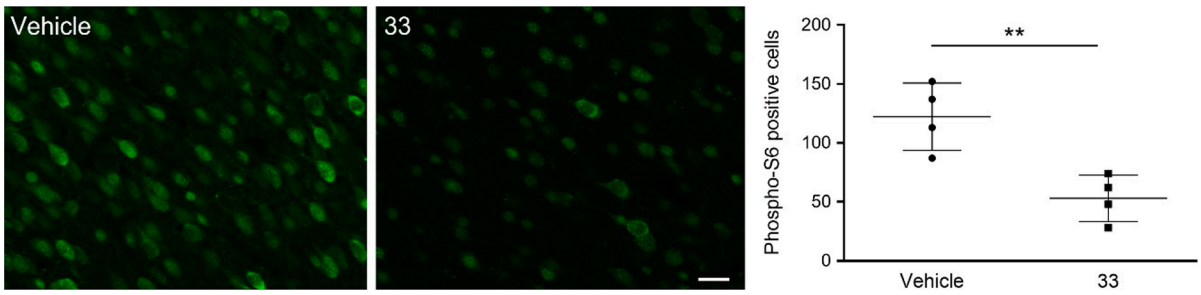

Fig. 4. Compound **33** suppresses phosphorylation of S6 in the prefrontal cortex, a downstream target for mTOR signaling. Scale bar: 20 μm. ** $p < 0.01$ (unpaired *t*-test).

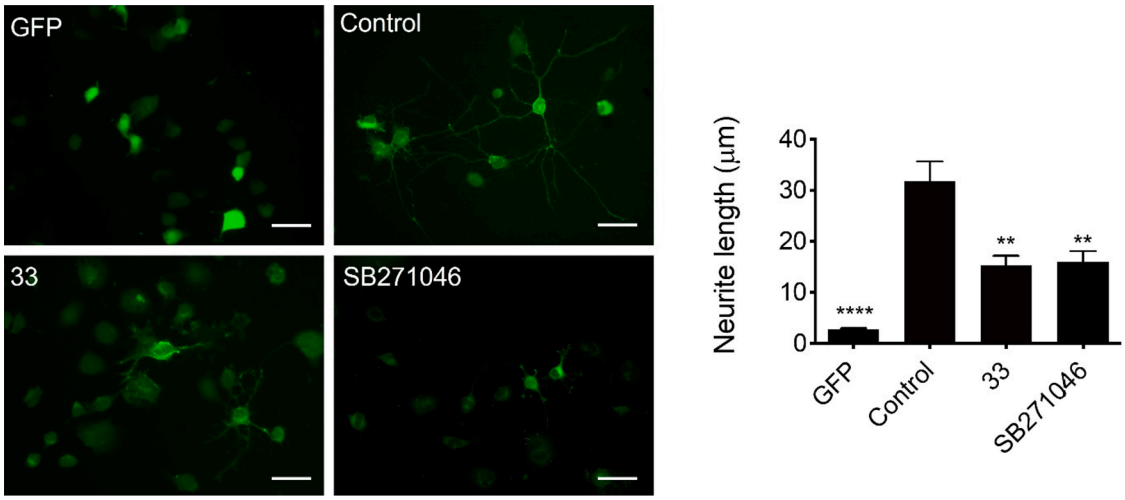

Fig. 3. Inhibition of neurite extension in NG108-15 cells expressing a constitutively active 5-HT_6R by compound **33** and SB-271046. Neurite length was measured in NG108-15 cells expressing a plasmid encoding a GFP-tagged 5-HT_6R or GFP alone, after a 24 h treatment with either DMSO (control), compound **33** (10^{-8} M), or SB-271046 (10^{-8} M). The histogram represents the mean neurite length ± SEM measured in each experimental condition. The results of three independent experiments is represented: ***$p < 0.001$ *vs.* cells expressing GFP; ANOVA followed by Student-Newman-Keuls test.

Table 5
Preliminary ADME/Tox assessment of compound **33**.

Assay Type	Compound 33
Microsomal stability[a]	Cl_{int} = 8.5 μL/min/mg
Chemical stability[b]	Stable at pH = 1 and 13
Solubility[c]	20 mg/ml
Neurotoxicity[d]	No IC_{50} = 27.4 μM
Hepatotoxicity[e]	No IC_{50} = 47.4 μM
Genotoxicity[f]	No

[a] Determined at a protein concentration of 0.4 mg/ml in RLM assay.
[b] Determined in aqueous solution of HCl (pH = 1) and NaOH (pH = 13) by HPLC analysis.
[c] Assessed in DPBS (pH = 7.4) at 20 °C in thermodynamic solubility assay.
[d-e] Cytotoxicity determined in SH-SY5Y[d] and HepG2[e] cellular models, when treated with tested compound **33** for 48 h.
[f] Assessed in the micronucleus assay using CHO-K1 cellular model.

induced anti-allodynic effect in a preclinical model of traumatic neuropathy of high translational value, i.e., SNL model [10], we chose to evaluate the *in vivo* activity of compound **33** in SNL rats. Sprague-Dawley male rats were subject to unilateral spinal nerve (L5) ligation. Two weeks later, the paw ipsilateral to nerve injury was tested with von Frey monofilaments to assess tactile allodynia. The allodynic rats (i.e., those presenting a reduction of paw withdrawal threshold) were intraperitoneally (*i.p.*) injected with either compound **33** (5 and 25 μmol/kg), PZ-1388 (25 μmol/kg) [10], or vehicle (water for injection, 5 mL/kg) and submitted again to von Frey hair application. Compound **33** (25 μmol/kg) significantly increased the 50% threshold at 30 to 90 min after administration and reached the maximal effect at 30–60 min after injection resulting, like PZ-1388 (25 μmol/kg), in a total abolition of SNL-induced tactile allodynia (Fig. 5A). The area under the curves (AUCs) of the 50% threshold variations confirmed the similar anti-allodynic effect of PZ-1388 and compound **33** (Fig. 5B).

3. Conclusions

In line with our objective to reposition 5-HT_6R inverse agonists for

Table 6
Pharmacokinetic parameters of compound **33**.

Parameters[a]	Compound 33	
	Plasma	Brain
$AUC_{0\rightarrow t}$ [ng · min/mL]	61,753	134,410
MRT [min]	197.6	227.5
$t_{0.5}$ [min]	349.1	1743
C_{max} [ng/mL] [ng/g][b]	216.6	436.6
t_{max} [min]	60	30
Vd/F [L/kg]	81	–

[a] Measured after *i.g.* gavage of dose 10 mg/kg; $t_{0.5}$ – terminal half-life; $AUC_{0\rightarrow t}$ – area under the curve from zero to last sampling time; MRT – mean residence time; C_{max} – maximum concentration; t_{max} – time to reach the maximum concentration; Vd/F – apparent volume of distribution.
[b] Concentration in brain; number of animals = 16.

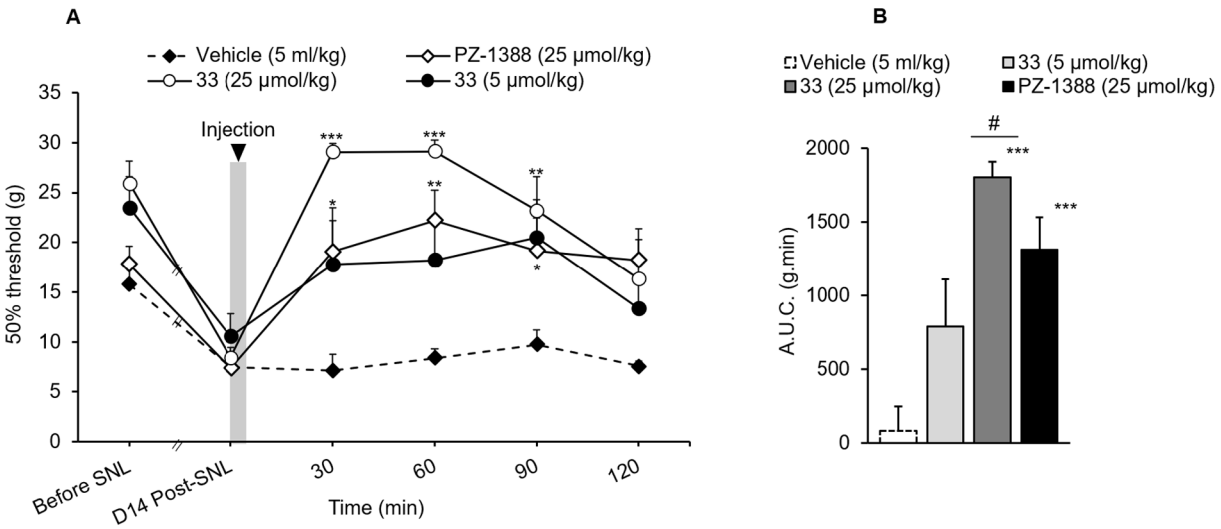

Fig. 5. Compound **33** produces anti-allodynic effect in rats SNL rats. **A)** Intraperitoneal administration of compound **33** (5 µmol/kg, n = 7 or 25 µmol/kg, n = 6) or PZ-1388 (25 µmol/kg, n = 6) but not vehicle (water for injection, n = 6) reduced tactile allodynia in SNL rats. Data represent mean ± SEM. $P(25, 192) = 1.680$; p = 0.0278; $^{\#\#\#}P < 0.001$ compared with values measured before SNL; $^{*}p < 0.05$, $^{**}p < 0.01$, $^{***}p < 0.001$ *vs* values measured before the drug/vehicle injection (D14 Post-SNL), by a 2-way RM ANOVA followed by a Tukey test. **B)** Area under the (A.U.C.) of paw withdrawal threshold variations in SNL rats. A.U.C. were calculated by the trapezoidal rule (in g.min). $^{***}P < 0.001$ *vs* vehicle, $^{\#}P < 0.05$ *vs* corresponding group, 1-way ANOVA followed by a Bonferroni test.

the treatment of neuropathic pain, we performed structural functionalization of the 2-phenyl-1*H*–pyrrole-3-carboxamide framework to provide a small library of 5-HT_6R ligands. Among the series of phenylsulfonyl derivatives of 2-aryl-1*H*-pyrrole-3-carboxamides, 2-(4-fluorophenyl)-1-[(3-chlorophenyl)sulfonyl]-*N*-(piperidin-4-yl)-1*H*-pyrrole-3-carboxamide (**33**) showed high affinity for 5-HT_6R (K_i = 23 nM) and high selectivity over off-target receptors. The *in vitro* evaluation of functional activity of **33** revealed the inverse agonism effect at Gs signaling and Cdk5-dependent neurite growth. Importantly, compound **33** also inhibited mTOR kinase under the control of constitutively active 5-HT_6R. This compound showed no cytotoxicity, had high metabolic stability, and easily penetrated into the brain. Finally, compound **33** exhibited rapid and potent *in vivo* anti-allodynic effect compatible with its pharmacokinetics in SNL-induced neuropathy in rats, an experimental model of traumatic neuropathic pain of high translational value. Considering the limitations of the currently available therapies, the ability of 5-HT_6R inverse agonists to alleviate painful symptoms in different models of traumatic neuropathy as well as neuropathies induced by metabolic disorders (e.g., diabetes) and chemotherapies (e.g., anticancer drugs) certainly warrants further investigation.

4. Experimental part

4.1. Chemistry

4.1.1. General methods

Chemicals and solvents were purchased from commercial suppliers (Sigma-Aldrich, Fluorochem, Across, TCI chemicals or Chempur) and used as received. Continuous flow experiments were conducted using a Uniqsis Flowsyn Multi-X equipment. Column chromatography was performed using silica gel Merck 60 (70–230 mesh ASTM) or Biotage Isolera flash chromatography system using Biotage SNAP HP-Sil cartridges.

Mass spectra were recorded on a UPLC-MS/MS system consisted of a Waters ACQUITY UPLC coupled to a Waters TQD mass spectrometer or LC-MS with ESI using Waters Alliance 2695 as LC, coupled to a Waters ZQ mass spectrometer with electrospray source, a simple quadrupole analyzer and a UV Waters 2489 detector. The UPLC/MS purity of all synthesized compounds was determined to be > 96%. Retention times (t_R) were provided in minutes. HRMS analyses were conducted using an UPLC Acquity H-Class from Waters hyphenated to a Synapt G2-S mass spectrometer with a dual ESI source from Waters.

^{1}H and ^{13}C NMR spectra were recorded on a Varian BB 200 (300 and 75 MHz), Bruker Avance III (400 MHz and 101 MHz) or JEOL JNM-ECZR500 RS1 (500 and 126 MHz). Chemical shifts were reported in parts per million (ppm), and the residual solvent peak ($CDCl_3$ or CD_3OD) was used as an internal reference. Coupling constants (*J*) were reported in Hertz (Hz), and multiplicity was indicated as follows: br s. (broad singlet), s (singlet), d (doublet), t (triplet), q (quartet), dd (doublet of doublets), dt (doublet of triplets), td (triplet of doublets), ddd (doublet of doublets of doublets), m (multiplet).

The synthesis of starting 2-substituted-1*H*-pyrrole-3-carboxylic acids was performed according to the previously described procedures [28,30,41], except for **7j–k**, for which the detailed synthetic procedure is placed in Supplementary Information. The characterization of selected final compounds **13, 14**, **18**, **20**, **27**, **30**, **32**, **33**, **36**, **37** is presented below, while the spectroscopic data of all intermediates as well as final compounds excluded from the main manuscript are reported in the Supplementary Information.

4.1.2. General procedure for amidation (*8a–r*)

The carboxylic acid **7a–k** (1 equiv.), 1-hydroxybenzotriazole (HOBt) (1.2 equiv) and benzotriazole-1-yl-oxy-tris-(dimethylamino)-phosphonium hexafluorophosphate (BOP) (1.2 equiv.) were dissolved in DMF, followed by addition of triethylamine (3 equiv.). The resulting mixture was stirred for 30 min. Next, the appropriate amine (1.2 equiv.) was added and left to react overnight. The mixture was diluted with EtOAc and washed three times with water and brine, dried over Na_2SO_4 and concentrated under vacuum. The crude product was purified on silica gel (the eluting system is indicated for each compound together with characterisation data).

4.1.3. General procedure for sulfonylation providing the final compounds *9–37*

The carboxamide **8a–r** (1 equiv.) was dissolved in CH_2Cl_2 and treated with phosphazene base P_1-*t*-Bu-tris(tetramethylene) (BTPP) (1.2 equiv.). After cooling down (ice-bath), the appropriate phenylsulfonyl chloride (1.2 equiv.) or 3-chlorobenzyl bromide (for **37**) was added and the mixture was stirred for 3 h. Then, the solvent was evaporated and the remaining crude product was purified on silica gel (the eluting system is

indicated for each compound together with characterization data). Further removal of Boc-protecting group was performed using 1.25 M methanolic HCl to give the final products (**9**–**37**) as hydrochloride salts after evaporation.

4.1.4. Characterization data for selected final compounds : ***13, 14, 18, 20, 27, 33, 36, 37***

*4.1.4.1. 2-Phenyl-1-(phenylsulfonyl)-N-(piperidin-4-yl)-1H-pyrrole-3-carboxamide hydrochloride (**13**).* White solid, 0.14 g (yield 84%); UPLC/MS purity 100%, t_R = 4.27, $C_{22}H_{24}ClN_3O_3S$, MW 445.96. ^{1}H NMR: (500 MHz, CD_3OD) δ ppm 1.41–1.51 (m, 2H), 1.84 (dd, *J* = 14.3, 3.4 Hz, 2H), 2.91–3.00 (m, 2H), 3.10–3.18 (m, 2H), 3.78–3.86 (m, 1H), 6.69 (d, *J* = 3.4 Hz, 1H), 7.06 (dd, *J* = 8.2, 1.3 Hz, 2H), 7.30–7.36 (m, 4H), 7.39–7.47 (m, 3H), 7.57 (d, *J* = 3.4 Hz, 1H), 7.60–7.65 (m, 1H). ^{13}C NMR (126 MHz, CD_3OD) δ ppm 29.1, 43.9, 45.4, 111.8, 123.9, 124.9, 128.7, 128.9, 130.5, 130.6, 130.8, 133.3, 135.7, 136.2, 139.6, 166.2. Monoisotopic Mass: 409.15, $[M+H]^+$ 410. HRMS calculated for $C_{22}H_{23}N_3O_3S$ 410.1494; found: 410.1537.

*4.1.4.2. 2-Phenyl-1-(phenylsulfonyl)-N-((1R,5S)-8-azabicyclo[3.2.1] octan-3-yl)-1H-pyrrole-3-carboxamide hydrochloride (**14**).* White solid, 0.08 g (yield 70%); UPLC/MS purity 100%, t_R = 4.49, $C_{24}H_{26}ClN_3O_3S$, MW 472.00. ^{1}H NMR: (500 MHz, CD_3OD) δ ppm 1.20–1.27 (m, 2H), 1.68–1.79 (m, 4H), 2.09–2.16 (m, 2H), 3.77 (br. s., 2H), 3.90–3.96 (m, 1H), 6.67 (d, *J* = 3.4 Hz, 1H), 7.11 (dd, *J* = 8.0, 1.2 Hz, 2H), 7.30–7.33 (m, 2H), 7.35 (t, *J* = 7.7 Hz, 2H), 7.39–7.44 (m, 2H), 7.45–7.51 (m, 1H), 7.59 (d, *J* = 3.7 Hz, 1H), 7.60–7.65 (m, 1H). ^{13}C NMR (126 MHz, $CDCl_3$) δ ppm 25.6, 33.0, 41.3, 41.4, 54.3, 111.6, 123.3, 124.3, 128.0, 128.8, 129.9, 130.0, 130.5, 132.9, 134.2, 135.1, 138.8, 166.3. Monoisotopic Mass: 435.16, $[M+H]^+$ 436.

*4.1.4.3. 2-Phenyl-1-[(3-chlorophenyl)sulfonyl]-N-(piperidin-4-yl)-1H-pyrrole-3-carboxamide Hydrochloride (**18**).* White solid, 0.13 g (yield 74%); UPLC/MS purity 100%, t_R = 4.78, $C_{22}H_{23}Cl_2N_3O_3S$, MW 480.40. ^{1}H NMR (400 MHz, CD_3OD) δ ppm 1.48 (dtd, *J* = 14.4, 10.9, 10.9, 3.9 Hz, 2H) 1.84–1.92 (m, 2H) 2.95–3.03 (m, 2H) 3.17 (dt, *J* = 13.3, 3.7 Hz, 2H) 3.85 (tt, *J* = 10.3, 4.0 Hz, 1H) 6.73 (d, *J* = 3.5 Hz, 1H) 7.09–7.11 (m, 1H) 7.11–7.13 (m, 1H) 7.19 (t, *J* = 1.9 Hz, 1H) 7.35–7.41 (m, 3H) 7.44–7.53 (m, 2H) 7.61 (d, *J* = 3.5 Hz, 1H) 7.67 (ddd, *J* = 8.0, 2.1, 1.1 Hz, 1H). ^{13}C NMR (101 MHz, CD_3OD) δ ppm 29.2, 43.9, 45.5, 112.1, 124.0, 125.2, 127.0, 128.8, 129.0, 130.5, 130.9, 132.4, 133.4, 135.8, 136.2, 136.3, 141.0, 166.1. Monoisotopic Mass: 443.11, $[M+H]^+$ 444. HRMS calculated for $C_{22}H_{22}ClN_3O_3S$ 444.1070; found: 444.1147.

*4.1.4.4. 2-Phenyl-1-[(3,4-dichlorophenyl)sulfonyl]-N-(piperidin-4-yl)-1H-pyrrole-3-carboxamide hydrochloride (**20**).* White solid, 0.07 g (yield 72%); UPLC/MS purity 100%, t_R = 5.30, $C_{22}H_{22}Cl_3N_3O_3S$, MW 514.85. ^{1}H NMR: (500 MHz, CD_3OD) δ ppm 1.40–1.53 (m, 1H), 1.79–1.88 (m, 1H), 2.94 (t, *J* = 11.3 Hz, 2H), 3.08–3.19 (m, 1H), 3.77–3.86 (m, 1H), 6.70 (d, *J* = 3.4 Hz, 1H), 7.08 (d, *J* = 7.2 Hz, 2H), 7.25 (d, *J* = 2.3 Hz, 1H), 7.29–7.37 (m, 3H), 7.47 (t, *J* = 7.7 Hz, 1H), 7.56 (d, *J* = 3.4 Hz, 1H), 7.61 (d, *J* = 8.6 Hz, 1H). ^{13}C NMR (126 MHz, CD_3OD) δ ppm 27.7, 42.5, 44.0, 110.8, 122.5, 123.9, 126.8, 127.5, 129.0, 129.4, 129.5, 131.5, 131.9, 133.1, 134.6, 137.6, 139.0, 164.6. Monoisotopic Mass: 477.07, $[M+H]^+$ 478. HRMS calculated for $C_{22}H_{21}Cl_2N_3O_3S$ 478.0681; found: 478.0761.

*4.1.4.5. 2-(3-Methoxyphenyl)-1-(phenylsulfonyl)-N-(piperidin-4-yl)-1H-pyrrole-3-carboxamide hydrochloride (**27**).* White solid, 0.05 g (yield 57%); UPLC/MS purity 100%, t_R = 4.40, $C_{23}H_{26}ClN_3O_4S$, MW 475.99. ^{1}H NMR: (500 MHz, CD_3OD) δ ppm 1.38–1.49 (m, 2H), 1.84 (dd, *J* = 14.2, 3.3 Hz, 2H), 2.90–3.00 (m, 2H), 3.09–3.17 (m, 2H), 3.70 (s, 3H), 3.78–3.86 (m, 1H), 6.52–6.56 (m, 1H), 6.62 (d, *J* = 7.73 Hz, 1H), 6.67 (d, *J* = 3.7 Hz, 1H), 6.99 (dd, *J* = 8.3, 2.0 Hz, 1H), 7.21 (t, *J* = 7.9 Hz, 1H), 7.33–7.38 (m, 2H), 7.39–7.44 (m, 2H), 7.56 (d, *J* = 3.4 Hz, 1H), 7.61 (t, *J* = 7.4 Hz, 1H). ^{13}C NMR (126 MHz, CD_3OD) δ ppm 27.7, 42.4, 44.0, 54.5, 110.3, 115.2, 117.1, 122.4, 123.3, 124.1, 127.3, 128.6, 129.1, 130.3, 134.3, 134.4, 138.1, 159.0, 164.7. Monoisotopic Mass: 439.16, $[M+H]^+$ 440. HRMS calculated for $C_{23}H_{25}N_3O_4S$ 440.1599; found: 440.1646.

*4.1.4.6. 2-[4-Chlorophenyl]-1-(phenylsulfonyl)-N-(piperidin-4-yl)-1H-pyrrole-3-carboxamide hydrochloride (**30**).* White solid, 0.05 g (yield 63%), UPLC/MS purity 100%, t_R = 4.76, $C_{22}H_{23}Cl_2N_3O_3S$, MW 480.40. ^{1}H NMR: (300 MHz, CD_3OD) *δ* 1.49–1.62 (m, 2H), 1.91 (dd, *J* = 13.8, 2.6 Hz, 2H), 2.99 (td, *J* = 12.6, 2.9 Hz, 2H), 3.20–3.28 (m, 2H), 3.78–3.89 (m, 1H), 6.70 (d, *J* = 3.5 Hz, 1H), 6.99–7.02 (m, 1H), 7.02–7.05 (m, 1H), 7.27–7.31 (m, 1H), 7.31–7.34 (m, 1H), 7.35–7.41 (m, 2H), 7.41–7.49 (m, 2H), 7.59 (d, *J* = 3.5 Hz, 1H), 7.61–7.69 (m, 1H). ^{13}C NMR (126 MHz, CD_3OD) δ ppm 27.9, 42.7, 44.3, 110.3, 122.9, 123.6, 127.2, 127.3, 128.1, 129.2, 133.3, 133.8, 134.4, 135.0, 138.1, 164.6. Monoisotopic Mass: 443.11, $[M+H]^+$ 444. HRMS calculated for $C_{22}H_{22}ClN_3O_3S$ 444.1070; found: 444.1144.

*4.1.4.7. 2-(4-Fluorophenyl)-1-((3-fluorophenyl)sulfonyl)-N-(piperidin-4-yl)-1H-pyrrole-3-carboxamide hydrochloride (**32**).* White solid, 0.06 g (yield 75%), UPLC/MS purity 99%, t_R = 4.71, $C_{22}H_{22}ClF_2N_3O_3S$, MW 481.94. ^{1}H NMR: (500 MHz, CD_3OD) δ ppm 1.48–1.59 (m, 2H), 1.88 (dd, *J* = 14.2, 3.0 Hz, 2H), 2.97 (td, *J* = 12.7, 3.0 Hz, 2H), 3.21–3.27 (m, 2H), 3.83 (tt, *J* = 10.7, 3.9 Hz, 1H), 6.70 (d, *J* = 3.4 Hz, 1H), 7.01–7.10 (m, 5H), 7.20–7.23 (m, 1H), 7.41 (tdd, *J* = 8.4, 8.4, 2.5, 1.0 Hz, 1H), 7.45–7.51 (m, 1H), 7.57 (d, *J* = 3.4 Hz, 1H). ^{13}C NMR (126 MHz, CD_3OD) δ ppm 27.8, 42.7, 44.2, 110.6, 114.2 (d, *J* = 22.3 Hz), 114.5 (d, *J* = 26.0 Hz), 121.5 (d, *J* = 21.1 Hz), 122.8, 123.2 (d, *J* = 3.0 Hz), 123.9, 125.3 (d, *J* = 3.6 Hz), 131.5 (d, *J* = 7.9 Hz), 133.9, 134.0 (d, *J* = 8.4 Hz), 139.8 (d, *J* = 7.2 Hz), 161.1 (d, *J* = 251.1 Hz), 163.3 (d, *J* = 248.1 Hz), 164.5. Monoisotopic Mass: 445.13, $[M+H]^+$ 446.

*4.1.4.8. 2-(4-Fluorophenyl)-1-[(3-chlorophenyl)sulfonyl]-N-(piperidin-4-yl)-1H-pyrrole-3-carboxamide hydrochloride (**33**).* White solid, 0.09 g (yield 80%), UPLC/MS purity 100%, t_R = 4.91, $C_{22}H_{22}Cl_2FN_3O_3S$, MW 498.39. ^{1}H NMR: (500 MHz, CD_3OD) δ ppm 1.48–1.60 (m, 2H), 1.89 (dd, *J* = 14.2, 3.0 Hz, 2H), 2.97 (td, *J* = 12.6, 3.2 Hz, 2H), 3.21–3.27 (m, 2H), 3.79–3.87 (m, 1H), 6.71 (d, *J* = 3.4 Hz, 1H), 7.07 (d, *J* = 7.2 Hz, 4H), 7.18 (t, *J* = 1.9 Hz, 1H), 7.36 (dq, *J* = 7.9, 0.9 Hz, 1H), 7.45 (t, *J* = 8.0 Hz, 1H), 7.57 (d, *J* = 3.4 Hz, 1H), 7.63–7.67 (m, 1H). ^{13}C NMR (126 MHz, CD_3OD) δ ppm 27.9, 42.7, 44.2, 110.5, 114.3 (d, *J* = 22.3 Hz), 122.7, 123.9, 125.2 (d, *J* = 3.6 Hz), 125.5, 127.2, 131.0, 133.9, 134.1 (d, *J* = 8.5 Hz), 134.4, 134.9, 139.5, 163.5 (d, *J* = 248.7 Hz), 164.5. Monoisotopic Mass: 461.10, $[M+H]^+$ 462. HRMS calculated for $C_{22}H_{21}ClFN_3O_3S$ 462.0976; found: 462.1055.

*4.1.4.9. 2-(thien-2-yl)-1-((3-chlorophenyl)sulfonyl)-N-(piperidin-4-yl)-1H-pyrrole-3-carboxamide hydrochloride (**36**).* White solid, 0.06 g (yield 62%); UPLC/MS purity 99%, t_R = 4.69, $C_{20}H_{21}Cl_2N_3O_3S_2$, MW 486.43. ^{1}H NMR (300 MHz, CD_3OD) δ ppm 1.43–1.60 (m, 2H), 1.86–1.97 (m, 2H), 2.93–3.07 (m, 2H), 3.13–3.24 (m, 2H), 3.81–3.93 (m, 1H), 6.69 (d, *J* = 3.5 Hz, 1H), 7.07–7.11 (m, 1H), 7.14 (dd, *J* = 5 0.3, 3.5 Hz, 1H), 7.31–7.34 (m, 1H), 7.41–7.48 (m, 2H), 7.61 (dd, *J* = 5.3, 1.2 Hz, 1H), 7.63–7.69 (m, 2H). ^{13}C NMR (126 MHz, CD_3OD) δ ppm 27.7, 42.4, 44.0, 110.6, 123.5, 125.7, 126.3, 126.6, 127.3, 127.7, 128.7, 129.6, 130.9, 133.1, 134.4, 135.0, 139.3, 164.4. Monoisotopic Mass: 449.06, $[M+H]^+$ 450. HRMS calculated for $C_{20}H_{20}ClN_3O_3S_2$ 450.0635; found: 450.0739.

*4.1.4.10. 2-(4-Fluorophenyl)-1-(3-chlorobenzyl)-N-(piperidin-4-yl)-1H-pyrrole-3-carboxamide hydrochloride (**37**).* White solid, 0.09 g (yield 54%); UPLC/MS purity 100%, t_R = 5.07, $C_{23}H_{24}Cl_2FN_3O$, MW 448.36. ^{1}H NMR (500 MHz, CD_3OD) δ ppm 1.55–1.69 (m, 2H), 1.99 (d, *J* = 13.2 Hz, 2H), 3.01 (t, *J* = 11.2 Hz, 2H), 3.32 (br. s., 2H), 3.85–3.96 (m, 1H),

4.98 (s, 2H), 6.63 (d, J = 2.9 Hz, 1H), 6.73–6.80 (m, 2H), 6.89 (d, J = 3.2 Hz, 1H), 7.04–7.11 (m, 2H), 7.15–7.22 (m, 4H). ^{13}C NMR (126 MHz, CD_3OD) δ ppm 28.2, 42.9, 44.1, 49.8, 108.1, 114.9 (d, J = 21.7 Hz), 117.6, 122.3, 124.72, 126.3, 127.3, 127.8 (d, J = 3.6 Hz), 129.8, 132.8 (d, J = 8.5 Hz), 134.2, 134.8, 140.4, 162.9 (d, J = 246.3 Hz), 166.1. Monoisotopic Mass: 411.15, $[M+H]^+$ 412. HRMS calculated for $C_{23}H_{23}ClFN_3O$ 412.1514; found: 412.1593.

4.2. In vitro pharmacological evaluation

4.2.1. Radioligand binding assays

All experiments were performed in line with the previously published procedures [42–44], using HEK293 cells stably expressing human 5-HT_{1A}, 5-HT_6, 5-HT_{7b} and D_{2L} receptors or CHO-K1 cells with human serotonin 5-HT_{2A} receptor. For displacement studies the assay samples contained as radioligands (PerkinElmer, USA): 2.5 nM [^{3}H]-8-OH-DPAT (135.2 Ci/ mmol) for 5-HT_{1A}R; 1 nM [^{3}H]-ketanserin (53.4 Ci/mmol) for 5-HT_{2A}R; 2 nM [^{3}H]-LSD (83.6 Ci/mmol) for 5-HT_6R; 0.8 nM [^{3}H]-5-CT (39.2 Ci/mmol) for 5-HT_7R or 2.5 nM [^{3}H]-raclopride (76.0 Ci/mmol) for D_{2L}R. Each compound was tested in triplicate at 7 concentrations (10^{-10}–10^{-4} M). The inhibition constants (K_i) were calculated from the Cheng-Prusoff equation [45]. Detailed description is reported in the Supplementary Information (SI: 6).

4.2.2. Determination of functional activity at Gs signaling

4.2.2.1. Impact of compound 33 on cAMP production in 1321N1 cells.

The ability of compound **33** to inhibit 5-CT-induced production of cAMP was evaluated using 1321N1 cells expressing the human 5-HT_6R (PerkinElmer). Compound was tested in triplicate at 8 concentrations (10^{-11}–10^{-4} M). Total cAMP was measured using the LANCE cAMP detection kit (PerkinElmer), according to the manufacturer's protocol. Time-resolved fluorescence resonance energy transfer (TR-FRET) was detected by an Infinite M1000 Pro (Tecan) using instrument settings from LANCE cAMP detection kit manual. K_b values were calculated from Cheng–Prusoff equation [45]. Detailed description is reported in the Supplementary Information (SI: 7.1).

4.2.2.2. Impact of compound 33 on cAMP production in NG108-15 cells.

We used NG108-15 cells transiently transfected with 5-HT_6R and with the cAMP sensor CAMYEL (cAMP sensor using YFP-Epac-RLuc) [19,46]. Constitutive activity of the receptor was assessed through bioluminescence resonance energy transfer (BRET) measurement using a Mithras LB 940 plate reader (Berthold Technologies). cAMP production induces a conformational change of the probe, resulting in the decrease of the BRET signal emitted by the CAMYEL probe in cells expressing the receptor when compared to cells expressing the probe alone. This decrease was subsequently used as an index of 5-HT_6R constitutive activity at Gs signaling. The inverse agonist properties of compound **33** and SB–271046 were tested by measuring BRET signal after a 24 h treatment, as their capacity to restore a BRET signal equivalent to the one measured in cells expressing the probe alone. Detailed description is reported in the Supplementary Information (SI: 7.2).

4.2.3. Impact of compound 33 on Cdk5-dependent neurite growth

The impact of a 24 h treatment with DMSO (control), compound **33** or SB–271046 (10^{-8} M) was assessed in NG108-15 cells expressing either cytosolic GFP or a GFP-tagged 5-HT_6R. Inhibition of Cdk5-5-HT_6R induced neurite growth was assessed on cells imaged using an AxioImagerZ1 microscope equipped with epifluorescence (Zeiss). Neurite length was measured using the Neuron J plugin of the ImageJ software (NIH). Detailed description is reported in the Supplementary Information (SI: 8).

4.2.4. Impact of compound 33 on 5-HT_6R-operated mTOR pathway

Rat were injected with vehicle or compound **33** (6 mg/kg, *p.o.*). Two hours after injection, rats were deeply anesthetized with ketamine (80 mg/kg) and xylazine (20 mg/kg) and perfused transcardially with 250 mL NaCl solution (0.9%; 32C) until all remaining blood was removed. Next, the animals were perfused with 500 mL 4% PFA in 0.1 M phosphate-buffered saline (PBS). Brains were post-fixed overnight in the same solution and stored at 4 °C. Fifty μm-thick sections were cut with a vibratome (Leica) and stored at 4 °C in 0.1 M sodium phosphate buffer (PBS), permeabilized with 0.1% Triton X-100 for 20 min and incubated for 48 h at 4 °C with anti-phospho-Ser$^{240/244}$ S6 antibody (1:500, Cell Signaling Technology) in PBS containing 0.025% Triton X-100 and 20% goat serum. Sections were then incubated for 1 h with goat Cy3-conjugated anti-mouse antibody (1:500, Jackson Laboratory) in PBS containing 20% goat serum. Immunofluorescent staining was observed with a Zeiss Axiophot2 microscope equipped with epifluorescence and quantification of phospho-Ser$^{240/244}$-S6 positive cells was performed on 224 μm × 168 μm images.

4.3. Preliminary ADME/Tox in vitro and in vivo evaluation

4.3.1. In vitro metabolic stability studies

Metabolic stability of compound **33** (10 μM) was analysed in rat liver microsomes (RLMs), using previously reported procedures [28]. Samples were analysed using UPLC/MS (Waters Corporation, Milford, MA). All experiments were run in duplicates. Half-life time was evaluated using linear regression model using Graph Pad Prism software and intrinsic clearance was calculated from the equation Cl_{int} = (volume of incubation [μL]/protein in the incubation [mg]) $0.693/t_{1/2}$ [47]. Detailed description is reported in the Supplementary Information (SI: 9).

4.3.2. In vitro cytotoxicity studies

HepG2 (ATCC) hepatocarcinoma cells, SH-SY5Y (ATCC) neuroblastoma cells, and CHO-K1 (ATCC) the Chinese hamster ovary cells were maintained in a humidified incubator at 37 °C with 5% CO_2 in EMEM (HepG2, SH-SY5Y) or F-12 K Medium (CHO-K1) supplemented with 10% fetal bovine serum (FBS, Gibco, Ireland) and antibiotics (Lonza, Switzerland). Cells were seeded in 96-multiwell plates at a density of 10 000 (HepG2, SHSY-5Y) or 6000 (CHO-K1) cells per well. Cells were incubated with vehicle, compound **33**, or doxorubicin at final concentrations of 0–150 μM, and the plates were gently mixed. After 24 h (CHO-K1) or 48 h (HepG2, SH-SY-5Y) incubation 10 μL of 3-(4,5-dimethylthiazol-2-yl)-2,5-diphenyltetrazolium bromide (MTT) solution (5 mg/mL) was added to the medium and incubated for a 3 h in 37 °C Then, when black crystals of formazan appeared at the bottom of the wells, the medium was removed and DMSO was added to dissolve formazan. Absorbance was read on a multiwell reader (Spectra Max iD3, Molecular Devices, USA) at 570 nm. Cell viability was determined in % of viability measured in vehicle-treated cells (100%). Three separate repeats of the experiment were performed. IC_{50} was calculated using GraphPad Prism 7.0150. Doxorubicin hydrochloride (>95% purity), used as a reference cytotoxic compound, was purchased from Enzo Life Sciences, USA.

4.3.3. In vitro genotoxicity studies

Micronucleus assay. For the test, CHO-K1 cells (1×10^6) were seeded in 25 mm^2 culture flasks and allowed to grow for 24 h (37 °C, 5% CO_2), then treated with different concentrations of compound **33**, mitomycin C (MMC) (Sigma Aldrich) (0.5 μg/mL, positive control) or water (vehicle control). After 24 h of treatment, medium containing cytochalasin B (CytB) (Sigma Aldrich, Darmstadt, Germany) (4.5 μg/mL) was added and incubation was continued for the next 24 h. After trypsinization, the cells were centrifuged and the supernatant was discarded. Then, CHO-K1 cells were briefly exposed to 1% ice-cold sodium citrate (Chempur) and fixed with methanol:acetic acid (3:1; *v/v*), together with 4 drops of

formaldehyde. The cell suspension was centrifuged (5 min, 1000 rpm), the supernatant was discarded, and the pellet was fixed in fixative mixture for two more times, without the addition of formaldehyde. Following fixation, the slides were prepared and dyed with Giemsa dye (1:20 in phosphate buffer) for 5 min [48–50]. Cells were analyzed using a microscope with a magnification of 40 × . The following parameters were analyzed: number of micronuclei (MN), dicentric bridges (DB) and nuclear buds (NB) per 1000 examined binuclear cells, and the nuclear division index (NDI). NDI was calculated using the formula: [(1 × MOC) + (2 × BC) + (3 × MUC)]/*N*, where MOC is the number of mononuclear cells, BC is the number of binuclear cells, MUC represents the number of multinuclear cells, and *N* is the total number of scored cells [49,50]. Experiment was conducted two times in two repetition for each condition.

4.3.4. *In vivo pharmacokinetic studies*

General conditions for pharmacokinetic studies is reported in the Supplementary Information (SI: 10). To determine the concentration of compound 33 in plasma and brain, an original method was developed using a high-performance liquid chromatography coupled to tandem mass spectrometry (LC-ESI/MS/MS). The method was validated according to FDA and EMA guidelines for bioanalytical method validation, in terms of method linearity, precision, accuracy, recovery and matrix effect [51].

4.3.4.1. Sample preparation. Prior to chromatographic separation, plasma samples and brain homogenates were purified by protein precipitation with acetonitrile cooled to 4 °C. Whole brains were used to prepare the brain tissue homogenates, which were carefully weighed beforehand, and homogenised using an electric homogeniser after the addition of phosphate buffer (pH 7.4) at a ratio of 1:2.5. For the determination of the concentration of compound 33, a 100 µL of rat plasma or brain homogenate was transferred to 2 mL Eppendorf tubes, and a 5 µL of the internal standard (IS, PH002437, Merck, Darmstadt, Germany) at a concentration of 5 µg/mL was added, thoroughly vortex-mixed for 10 s, whereupon 200 uL of acetonitrile was used to precipitate the proteins. The sample thus prepared was shaken for 20 min, then centrifuged (28,672 × g) for 10 min at 4 °C. After centrifugation, 200 uL of supernatants were collected from the upper layer, and transferred to a chromatography vials in which the inserts had previously been placed. Thereafter 20 uL of the prepared sample was injected on the chromatography column.

4.3.4.2. Animals. Evaluation of the pharmacokinetic profile of compound **33** was performed in Wistar rats (16 male, 8-week-old, weighing between 200 and 220 g each), purchased from the Animal House at the Faculty of Pharmacy, Jagiellonian University Medical College, Krakow (Poland). Rats were housed in standard polycarbonate cages (four animals per cage) with maintaining constant environmental conditions, in terms of relative humidity 50%–60%, temperature 22 ± 2 °C, normal 12-h light–dark cycle (7 a.m. to 7p.m. light). The animals were given standard rodent chow and water *ad libitum*. Compound **33** dissolved in PBS saline (pH 7.4) was given intragastrically to each animal at a dose of 6 mg/kg, whereupon the animals were sacrificed by decapitation in deep anasthesia after *i.p.* injections of 50 mg/kg ketamine plus 8 mg/kg xylazine at specific time-points: 30 min (n = 4), 60 min (n = 4), 90 min (n = 4) and 120 min (n = 4). The blood samples were drawn from each rat into heparinized tubes, and centrifuged at 3000 × *g* for 10 min to obtain plasma. In the final step, following the animals' euthanasia, the whole brain from each individuals was collected. Both plasma and brain samples were protected from degradation by freezing at temp. at − 80 °C. All experimental procedures were carried out in accordance with EU Directive 2010/63/EU and approved by the I Local Ethics Committee for Experiments on Animals of the Jagiellonian University in Krakow, Poland (No 83/2018).

4.4. *In vivo assessment of neuropathic pain-alleviating activity*

Male Sprague-Dawley rats weighting 150–175 g were purchased from Janvier Labs (Le Genest-Saint-Isle, France). Animals were housed four per cage under standard laboratory conditions and maintained on a 12 h:12 h light/dark cycle in specific pathogen free area. Water and food were available ad libidum. The experiments involving animals were conducted in accordance with the NC3R ARRIVE rules [52]. All prodecures were approved by local Ethics Committee of Auvergne (C2EA, France) and by the French Ministry of Higher Education and Innovation (authorization N° 2018111617333273 V5).

Unilateral traumatic neuropathy was induced by spinal nerve ligation according to the method described by Chung [53]. Briefly, rats were anesthetized with xylazine (10 mg/kg, intraperitoneal) and ketamine (75 mg/kg, i.p.). Under aseptic conditions, the left L5 spinal nerve was exposed and ligated with a nonabsorbable 5–0 braided silk thread. The muscle and skin were then sutured and the rats received a s.c. injection of meloxicam (non-steroidal anti-inflammatory drug) to reduce the post-surgery pain and inflammation. The animals were allowed to recover for the next 14 days and were monitored daily to insure good health.

Tactile allodynia was assessed using the von Frey hair test [54].The experimenter got the animals habituated to the testing environment 1 h before baseline. Each rat was confined in clear plexiglas compartment placed on an elevated metal mesh floor. A series of 8 Von Frey monofilaments were applied perpendicularly to the central plantar surface of the ipsilateral (side of surgery) hind paw for 5 s in ascending order of force (1.4 to 26 g). Paw withdrawal or licking was considered as a positive response and the next weaker filament was applied. In case of no paw withdrawal or licking, the next stronger filament was applied. This paradigm continued until four measurements have been obtained after an initial change of behavior, or until four consecutive negative responses or five consecutive positive responses. The 50 % response threshold was calculated using the Up-Down method and Dixon's formulae [55].

Drugs were blindly administrated according to the method of blocks and using a randomization procedure. Different animals were used in each experiment. At the end of the experiments, the animals were euthanized by progressive carbon dioxide inhalation (10–30%/min).

Declaration of Competing Interest

The authors declare that they have no known competing financial interests or personal relationships that could have appeared to influence the work reported in this paper.

Acknowledgments

The authors acknowledge the financial support from the National Science Centre, Poland (grant no. 2016/21/B/NZ7/01742), Priority Research Area qLife: "Excellence Initiative – Research University" at the Jagiellonian University, statutory activity of Jagiellonian University Medical College and Polish Academy of Sciences (Maj Institute of Pharmacology), PHC Polonium programme, Centre National de la Recherche Scientifique (CNRS) and Université de Montpellier. FJ, SL, AE and CC were financially supported by the Agence Nationale de la Recherche (ANR, ANR-18-CE18-0018), the program "Investissements d'Avenir'' (16-IDEX-0001 CAP 20-25), the Institut National de la Santé et de la Recherche Médicale (INSERM), Université Clermont Auvergne, and the Auvergne-Rhône-Alpes Region (France). SCD and PM were supported by grants from INSERM, CNRS, Montpellier University of Excellence (iSITE MUSE), the French Foundation for Medical Research (FRM) and ANR (ANR-17-CE16-0013-01, ANR-17-CE16-0010-01, and ANR-19-CE18-0018-02). MD thanks French Embassy in Poland for the French Government Scholarships. The authors thank Dr. Paweł Żmudzki for thermodynamic solubility assessment and Emeline Tamayo for her technical assistance.

Appendix A. Supplementary data

Supplementary data to this article can be found online at https://doi.org/10.1016/j.bioorg.2021.105218.

References

[1] O. van Hecke, S.K. Austin, R.A. Khan, B.H. Smith, N. Torrance, Neuropathic pain in the general population: a systematic review of epidemiological studies, Pain. 155 (2014) 654–662, https://doi.org/10.1016/j.pain.2013.11.013.

[2] C. Chenaf, J. Delorme, N. Delage, D. Ardid, A. Eschalier, N. Authier, Prevalence of chronic pain with or without neuropathic characteristics in France using the capture-recapture method: a population-based study, Pain. 159 (2018) 2394–2402, https://doi.org/10.1097/j.pain.0000000000001347.

[3] R.D. Treede, T.S. Jensen, J.N. Campbell, G. Cruccu, J.O. Dostrovsky, J.W. Griffin, P. Hansson, R. Hughes, T. Nurmikko, J. Serra, Neuropathic pain: redefinition and a grading system for clinical and research purposes, Neurology. 70 (2008) 1630–1635, https://doi.org/10.1212/01.wnl.0000282763.29778.59.

[4] T.S. Jensen, R. Baron, M. Haanpää, E. Kalso, J.D. Loeser, A.S.C. Rice, R.-D. Treede, A new definition of neuropathic pain, Pain. 152 (2011) 2204–2205, https://doi.org/10.1016/j.pain.2011.06.017.

[5] S.R.A. Alles, P.A. Smith, Etiology and pharmacology of neuropathic pain, Pharmacol. Rev. 70 (2018) 315–347, https://doi.org/10.1124/pr.117.014399.

[6] P.R. Kamerman, A.L. Wadley, K. Davis, A. Hietaharju, P. Jain, A. Kopf, A.C. Meyer, S.N. Raja, A.S.C. Rice, B.H. Smith, R.D. Treede, P.J. Wiffen, World Health Organization (WHO) essential medicines lists: where are the drugs to treat neuropathic pain? Pain. 156 (2015) 793–797, https://doi.org/10.1097/01.j.pain.0000460356.94374.a1.

[7] N.B. Finnerup, N. Attal, S. Haroutounian, E. McNicol, R. Baron, R.H. Dworkin, I. Gilron, M. Haanpaa, P. Hansson, T.S. Jensen, P.R. Kamerman, K. Lund, A. Moore, S.N. Raja, A.S. Rice, M. Rowbotham, E. Sena, P. Siddall, B.H. Smith, M. Wallace, Pharmacotherapy for neuropathic pain in adults: systematic review, meta-analysis and updated NeuPSIG recommendations, Lancet Neurol. 14 (2015) 162–173, https://doi.org/10.1016/S1474-4422(14)70251-0.

[8] Q.Q. Liu, X.X. Yao, S.H. Gao, R. Li, B.J. Li, W. Yang, R.J. Cui, Role of 5-HT receptors in neuropathic pain: potential therapeutic implications, Pharmacol. Res. 159 (2020), 104949, https://doi.org/10.1016/j.phrs.2020.104949.

[9] N.M. Barnes, G.P. Ahern, C. Becamel, J. Bockaert, M. Camilleri, S. Chaumont-Dubel, S. Claeysen, K.A. Cunningham, K.C. Fone, M. Gershon, G.D. Giovanni, N.M. Goodfellow, A.L. Halberstadt, R.M. Hartley, G. Hassaine, K. Herrick-Davis, R. Hovius, E. Lacivita, E.K. Lambe, M. Leopoldo, F.O. Levy, S.C.R. Lummis, P. Marin, L. Maroteaux, A.C. McCreary, D.L. Nelson, J.F. Neumaier, A. Newman-Tancredi, H. Nury, A. Roberts, B.L. Roth, A. Roumier, G.J. Sanger, M. Teitler, T. Sharp, C.M. Villalón, H. Vogel, S.W. Watts, D. Hoyer, International Union of Basic and Clinical Pharmacology. CX. Classification of Receptors for 5-hydroxytryptamine; Pharmacology and Function, Pharmacol Rev. 73 (2021) 310–520. https://doi.org/10.1124/pr.118.015552.

[10] P.Y. Martin, S. Doly, A.M. Hamieh, E. Chapuy, V. Canale, M. Drop, S. Chaumont-Dubel, X. Bantreil, F. Lamaty, A.J. Bojarski, P. Zajdel, A. Eschalier, P. Marin, C. Courteix, mTOR activation by constitutively active serotonin 6 receptors as new paradigm in neuropathic pain and its treatment, Prog. Neurobiol. 193 (2020), 101846, https://doi.org/10.1016/j.pneurobio.2020.101846.

[11] S. Chaumont-Dubel, V. Dupuy, J. Bockaert, C. Bécamel, P. Marin, The 5-HT$_6$ receptor interactome: New insight in receptor signaling and its impact on brain physiology and pathologies, Neuropharmacology. 172 (2020), 107839, https://doi.org/10.1016/j.neuropharm.2019.107839.

[12] R. Kohen, L.A. Fashingbauer, D.E. Heidmann, C.R. Guthrie, M.W. Hamblin, Cloning of the mouse 5-HT$_6$ serotonin receptor and mutagenesis studies of the third cytoplasmic loop, Brain Res. Mol. Brain Res. 90 (2001) 110–117, https://doi.org/10.1016/s0169-328x(01)00090-0.

[13] W. Deraredj Nadim, S. Chaumont-Dubel, F. Madouri, L. Cobret, M.L. De Tauzia, P. Zajdel, H. Bénédetti, P. Marin, S. Morisset-Lopez, Physical interaction between neurofibromin and serotonin 5-HT$_6$ receptor promotes receptor constitutive activity, Proc. Natl. Acad. Sci. U.S.A. 113 (2016) 12310–12315, https://doi.org/10.1073/pnas.1600914113.

[14] V.E. Abraira, E.D. Kuehn, A.M. Chirila, M.W. Springel, A.A. Toliver, A. L. Zimmerman, L.L. Orefice, K.A. Boyle, L. Bai, B.J. Song, K.A. Bashista, T. G. O'Neill, J. Zhuo, C. Tsan, J. Hoynoski, M. Rutlin, L. Kus, V. Niederkofler, M. Watanabe, S.M. Dymecki, S.B. Nelson, N. Heintz, D.I. Hughes, D.D. Ginty, The cellular and synaptic architecture of the mechanosensory dorsal horn, Cell. 168 (2017) 295–310, https://doi.org/10.1016/j.cell.2016.12.010.

[15] I.E.M. de Jong, A. Mørk, Antagonism of the 5-HT$_6$ receptor - preclinical rationale for the treatment of Alzheimer's disease, Neuropharmacology. 125 (2017) 50–63, https://doi.org/10.1016/j.neuropharm.2017.07.010.

[16] H. Ferrero, M. Solas, P.T. Francis, M.J. Ramirez, Serotonin 5-HT$_6$ receptor antagonists in Alzheimer's Disease: therapeutic rationale and current development status, CNS Drugs. 31 (2017) 19–32, https://doi.org/10.1007/s40263-016-0399-3.

[17] P. Zajdel, K. Marciniec, G. Satała, V. Canale, T. Kos, A. Partyka, M. Jastrzębska-Więsek, A. Wesołowska, A. Basińska-Ziobroń, J. Wójcikowski, W.A. Daniel, A. J. Bojarski, P. Popik, N1-Azinylsulfonyl-1H-indoles: 5-HT$_6$ receptor antagonists with procognitive and antidepressant-like properties, ACS Med. Chem. Lett. 7 (2016) 618–622, https://doi.org/10.1021/acsmedchemlett.6b00056.

[18] D. Vanda, M. Soural, V. Canale, S. Chaumont-Dubel, G. Satała, T. Kos, P. Funk, V. Fülöpová, B. Lemrová, P. Koczurkiewicz, E. Pękala, A.J. Bojarski, P. Popik, P. Marin, P. Zajdel, Novel non-sulfonamide 5-HT$_6$ receptor partial inverse agonist in a group of imidazo[4,5-b]pyridines with cognition enhancing properties, Eur. J. Med. Chem. 144 (2018) 716–729, https://doi.org/10.1016/j.ejmech.2017.12.053.

[19] D. Vanda, V. Canale, S. Chaumont-Dubel, R. Kurczab, G. Satała, P. Koczurkiewicz-Adamczyk, M. Krawczyk, W. Pietruś, K. Blicharz, E. Pękala, A.J. Bojarski, P. Popik, P. Marin, M. Soural, P. Zajdel, Imidazopyridine-based 5-HT$_6$ receptor neutral antagonists: impact of N1-benzyl and N1-phenylsulfonyl fragments on different receptor conformational states, J. Med. Chem. 64 (2021) 1180–1196, https://doi.org/10.1021/acs.jmedchem.0c02009.

[20] J.B. Pineda-Farias, P. Barragán-Iglesias, A. Valdivieso-Sánchez, J. Rodríguez-Silverio, F.J. Flores-Murrieta, V. Granados-Soto, H.I. Rocha-González, Spinal 5-HT$_4$ and 5-HT$_6$ receptors contribute to the maintenance of neuropathic pain in rats, Pharmacol. Rep. 69 (2017) 916–923, https://doi.org/10.1016/j.pharep.2017.04.001.

[21] V.N. Devegowda, J.-R. Hong, S. Cho, E.J. Lim, H. Choo, G. Keum, H. Rhim, G. Nam, Synthesis and the 5-HT$_6$ receptor antagonistic effect of 3-arylsulfonylamino-5,6-dihydro-6-substituted pyrazolo[3,4]pyridinones for neuropathic pain treatment, Bioorg. Med. Chem. Lett. 23 (2013) 4696–4700, https://doi.org/10.1016/j.bmcl.2013.05.100.

[22] J.R. Hong, H. Choo, G. Nam, Neuropathic pain-alleviating effects of pyrazole-conjugated arylsulfonamides as 5-HT$_6$ receptor antagonists, Bioorg. Med. Chem. Lett. 27 (2017) 4146–4149, https://doi.org/10.1016/j.bmcl.2017.07.031.

[23] B.M. Lutz, S. Nia, M. Xiong, Y.-X. Tao, A. Bekker, mTOR, a new potential target for chronic pain and opioid-induced tolerance and hyperalgesia, Mol. Pain. 11 (2015) 32, https://doi.org/10.1186/s12990-015-0030-5.

[24] D. Lyu, W. Yu, N. Tang, R. Wang, Z. Zhao, F. Xie, Y. He, H. Du, J. Chen, The mTOR signaling pathway regulates pain-related synaptic plasticity in rat entorhinal-hippocampal pathways, Mol. Pain. 9 (2013) 64, https://doi.org/10.1186/1744-8069-9-64.

[25] S.M. Géranton, L. Jiménez-Díaz, C. Torsney, K.K. Tochiki, S.A. Stuart, J.L. Leith, B. M. Lumb, S.P. Hunt, A rapamycin-sensitive signaling pathway is essential for the full expression of persistent pain states, J. Neurosci. 29 (2009) 15017–15027, https://doi.org/10.1523/JNEUROSCI.3451-09.2009.

[26] X. Wang, X. Li, B. Huang, S. Ma, Blocking mammalian target of rapamycin (mTOR) improves neuropathic pain evoked by spinal cord injury, Transl. Neurosci. 7 (2016) 50–55, https://doi.org/10.1515/tnsci-2016-0008.

[27] Z. Duan, J. Li, X. Pang, H. Wang, Z. Su, Blocking mammalian target of rapamycin (mTOR) alleviates neuropathic pain induced by chemotherapeutic bortezomib, Cell Physiol. Biochem. 48 (2018) 54–62, https://doi.org/10.1159/000491662.

[28] M. Drop, V. Canale, S. Chaumont-Dubel, R. Kurczab, G. Satała, X. Bantreil, M. Walczak, P. Koczurkiewicz-Adamczyk, G. Latacz, A. Gwizdak, M. Krawczyk, J. Gołębiowska, K. Grychowska, A.J. Bojarski, A. Nikiforuk, G. Subra, J. Martinez, M. Pawłowski, P. Popik, P. Marin, F. Lamaty, P. Zajdel, 2-Phenyl-1H-pyrrole-3-carboxamide as a new scaffold for developing 5-HT$_6$ receptor inverse agonists with cognition-enhancing activity, ACS Chem. Neurosci. 12 (2021) 1228–1240, https://doi.org/10.1021/acschemneuro.1c00061.

[29] J.N. Kim, H.J. Lee, K.Y. Lee, J.H. Gong, Regioselective allylic amination of the Baylis-Hillman adducts: an easy and practical access to the Baylis-Hillman adducts of N-tosylimines, Synlett. 1 (2002) 173–175, https://doi.org/10.1055/s-2002-19360.

[30] M. Drop, X. Bantreil, K. Grychowska, G.U. Mahoro, E. Colacino, M. Pawłowski, J. Martinez, G. Subra, P. Zajdel, F. Lamaty, Continuous flow ring-closing metathesis, an environmentally-friendly route to 2,5-dihydro-1H-pyrrole-3-carboxylates, Green Chem. 19 (2017) 1647–1652, https://doi.org/10.1039/C7GC00235A.

[31] A.S. Hogendorf, A. Hogendorf, R. Kurczab, J. Kalinowska-Tłuścik, P. Popik, A. Nikiforuk, M. Krawczyk, G. Satała, T. Lenda, J. Knutelska, R. Bugno, J. Staroń, W. Pietruś, M. Matłoka, K. Dubiel, R. Moszczyński-Pętkowski, J. Pieczykolan, M. Wieczorek, B. Pilarski, P. Zajdel, A.J. Bojarski, 2-Aminoimidazole-based antagonists of the 5-HT$_6$ receptor - A new concept in aminergic GPCR ligand design, Eur. J. Med. Chem. 179 (2019) 1–15, https://doi.org/10.1016/j.ejmech.2019.06.001.

[32] C. Routledge, S.M. Bromidge, S.F. Moss, G.W. Price, W. Hirst, H. Newman, G. Riley, T. Gager, T. Stean, N. Upton, S.E. Clarke, A.M. Brown, D.N. Middlemiss, Characterization of SB-271046: a potent, selective and orally active 5-HT$_6$ receptor antagonist, Br. J. Pharmacol. 130 (2000) 1606–1612, https://doi.org/10.1038/sj.bjp.0703457.

[33] K. Grychowska, G. Satała, T. Kos, A. Partyka, E. Colacino, S. Chaumont-Dubel, X. Bantreil, A. Wesołowska, M. Pawłowski, J. Martinez, P. Marin, G. Subra, A. J. Bojarski, F. Lamaty, P. Popik, P. Zajdel, Novel 1H-pyrrolo[3,2-c]quinoline based 5-HT$_6$ receptor antagonists with potential application for the treatment of cognitive disorders associated with Alzheimer's Disease, ACS Chem. Neurosci. 7 (2016) 972–983, https://doi.org/10.1021/acschemneuro.6b00090.

[34] V. Canale, K. Grychowska, R. Kurczab, M. Ryng, A.R. Keeri, G. Satała, A. Olejarz-Maciej, P. Koczurkiewicz, M. Drop, K. Blicharz, K. Piska, E. Pękala, P. Janiszewska, M. Krawczyk, M. Walczak, S. Chaumont-Dubel, A.J. Bojarski, P. Marin, P. Popik, P. Zajdel, A dual-acting 5-HT$_6$ receptor inverse agonist/MAO-B inhibitor displays glioprotective and pro-cognitive properties, Eur. J. Med. Chem. 208 (2020), 112765, https://doi.org/10.1016/j.ejmech.2020.112765.

[35] P. De Deurwaerdère, R. Bharatiya, A. Chagraoui, G. Di Giovanni, Constitutive activity of 5-HT receptors: Factual analysis, Neuropharmacology. 168 (2020), 107967, https://doi.org/10.1016/j.neuropharm.2020.107967.

[36] N. Hay, N. Sonenberg, Upstream and downstream of mTOR, Genes Dev. 18 (2004) 1926–1945, https://doi.org/10.1101/gad.1212704.

[37] J. Bockaert, P. Marin, mTOR in brain physiology and pathologies, Physiol. Rev. 95 (2015) 1157–1187, https://doi.org/10.1152/physrev.00038.2014.

[38] L. Lisi, P. Aceto, P. Navarra, C. Dello Russo, mTOR kinase: a possible pharmacological target in the management of chronic pain, Biomed. Res. Int. 2015 (2015), 394257, https://doi.org/10.1155/2015/394257.
[39] J.T. Xu, X. Zhao, M. Yaster, Y.X. Tao, Expression and distribution of mTOR, p70S6K, 4E-BP1, and their phosphorylated counterparts in rat dorsal root ganglion and spinal cord dorsal horn, Brain Res. 1336 (2010) 46–57, https://doi.org/10.1016/j.brainres.2010.04.010.
[40] W.Y. He, B. Zhang, W.C. Zhao, J. He, L. Zhang, Q.M. Xiong, J. Wang, H.B. Wang, Contributions of mTOR activation-mediated upregulation of synapsin II and neurite outgrowth to hyperalgesia in STZ-induced diabetic rats, ACS Chem. Neurosci. 10 (2019) 2385–2396, https://doi.org/10.1021/acschemneuro.8b00680.
[41] P. Zajdel, M. Drop, V. Canale, M. Pawłowski, G. Satała, A.J. Bojarski, G. Subra, J. Martinez, X. Bantreil, F. Lamaty, P.Y. Martin, C. Courteix, S. Chaumont-Dubel, P. Marin, Arylsulfonamides of 2-arylpyrrole-3-carboxamides for the treatment of CNS disorders (2020). WO2020117075A1.
[42] R. Kurczab, V. Canale, G. Satała, P. Zajdel, A.J. Bojarski, Amino acid hot spots of halogen bonding: A combined theoretical and experimental case study of the 5-HT_7 receptor, J. Med. Chem. 61 (2018) 8717–8733, https://doi.org/10.1021/acs.jmedchem.8b00828.
[43] A. Partyka, R. Kurczab, V. Canale, G. Satała, K. Marciniec, A. Pasierb, M. Jastrzębska-Więsek, M. Pawłowski, A. Wesołowska, A.J. Bojarski, P. Zajdel, The impact of the halogen bonding on D_2 and 5-HT_{1A}/5-HT_7 receptor activity of azinesulfonamides of 4-[(2-ethyl)piperidinyl-1-yl]phenylpiperazines with antipsychotic and antidepressant properties, Bioorg. Med. Chem. 25 (2017) 3638–3648, https://doi.org/10.1016/j.bmc.2017.04.046.
[44] P. Zajdel, T. Kos, K. Marciniec, G. Satała, V. Canale, K. Kamiński, M. Hołuj, T. Lenda, R. Koralewski, M. Bednarski, L. Nowiński, J. Wójcikowski, W.A. Daniel, A. Nikiforuk, I. Nalepa, P. Chmielarz, J. Kuśmierczyk, A.J. Bojarski, P. Popik, Novel multi-target azinesulfonamides of cyclic amine derivatives as potential antipsychotics with pro-social and pro-cognitive effects, Eur. J. Med. Chem. 145 (2018) 790–804, https://doi.org/10.1016/j.ejmech.2018.01.002.
[45] Y. Cheng, W.H. Prusoff, Relationship between the inhibition constant (K1) and the concentration of inhibitor which causes 50 per cent inhibition (I50) of an enzymatic reaction, Biochem. Pharmacol. 22 (1973) 3099–3108.
[46] L.I. Jiang, J. Collins, R. Davis, K.-M. Lin, D. DeCamp, T. Roach, R. Hsueh, R. A. Rebres, E.M. Ross, R. Taussig, I. Fraser, P.C. Sternweis, Use of a cAMP BRET sensor to characterize a novel regulation of cAMP by the sphingosine 1-phosphate/G13 pathway, J. Biol. Chem. 282 (2007) 10576–10584, https://doi.org/10.1074/jbc.M609695200.
[47] J.K. Singh, A. Solanki, Comparative in-vitro intrinsic clearance of imipramine in multiple species liver microsomes: human, rat, mouse and dog, J. Drug Metab. Toxicol. 3 (2012) 126, https://doi.org/10.4172/2157-7609.1000126.
[48] K. Żelazna, K. Rudnicka, S. Tejs, In vitro micronucleus test assessment of polycyclic aromatic hydrocarbons, Environ. Biotechnol. 7 (2011) 70–80.
[49] M.C. Oliveira, L.M.S. Lemos, R.G. de Oliveira, E.L. Dall'Oglio, P.T. de Sousa Júnior, D.T. de Oliveira Martins, Evaluation of toxicity of Calophyllum brasiliense stem bark extract by in vivo and in vitro assays, J. Ethnopharmacol. 155 (2014) 30–38, https://doi.org/10.1016/j.jep.2014.06.019.
[50] E. Pavan, A.S. Damazo, L.M.S. Lemos, B. Adzu, S.O. Balogun, K. Arunachalam, D.T. de O. Martins, Evaluation of genotoxicity and subchronic toxicity of the standardized leaves infusion extract of Copaifera malmei Harms in experimental models, J. Ethnopharmacol. 211 (2018) 70–77, https://doi.org/10.1016/j.jep.2017.09.027.
[51] EMA. Guideline on bioanalytical method validation guideline on bioanalytical method validation table of contents. EMA: Amsterdam, The Netherlands, 2012.
[52] C. Kilkenny, W.J. Browne, I.C. Cuthill, M. Emerson, D.G. Altman, Improving bioscience research reporting: The ARRIVE guidelines for reporting animal research, PLoS Biology. 8 (2010), e1000412, https://doi.org/10.1371/journal.pbio.1000412.
[53] S.H. Kim, J.M. Chung, An experimental model for peripheral neuropathy produced by segmental spinal nerve ligation in the rat, Pain. 50 (1992) 355–363, https://doi.org/10.1016/0304-3959(92)90041-9.
[54] S.R. Chaplan, F.W. Bach, J.W. Pogrel, J.M. Chung, T.L. Yaksh, Quantitative assessment of tactile allodynia in the rat paw, J. Neurosci. Methods. 53 (1994) 55–63, https://doi.org/10.1016/0165-0270(94)90144-9.
[55] W.J. Dixon, Efficient analysis of experimental observations, Annu. Rev. Pharmacol. Toxicol. 20 (1980) 441–462, https://doi.org/10.1146/annurev.pa.20.040180.002301.